scientific reports

Check for updates

OPEN

Determination of probability density, position and momentum uncertainties, and information theoretic measures using a class of inversely quadratic Yukawa potential

Etido P. Inyang[1,2]✉, A. E. L. Aouami[4], N. Ali[2,3], R. Endut[2,3]✉, N. R. Ali[5] & S. A. Aljunid[2,3]

This study utilizes the Nikiforov-Uvarov method to solve the Schrödinger equation for the class of inversely quadratic Yukawa potential (CIQYP), deriving both the energy equation and the normalized wave function. Shannon entropy and Fisher information in both position and momentum spaces are analyzed for low-energy states using the wave function. The Bialynicki-Birula-Mycielski and Stam-Cramer-Rao inequalities are satisfied for the Shannon and Fisher information entropies, illustrating the complementary uncertainties inherent in position and momentum in quantum mechanics. The study underscores the interplay between position and momentum Fisher entropies, reinforcing the Heisenberg uncertainty principle, which imposes limits on the precise simultaneous measurement of conjugate variables. Eigenvalues of the CIQYP for three diatomic molecules (N_2, O_2, and NO) are obtained using their respective data, revealing that the bound state energy spectra of these diatomic molecules increase as both the principal quantum number and angular momentum quantum number rise. Expectation values were numerically determined, and the potential model simplifies to the Kratzer potential under specific boundary conditions, thereby ensuring analytical accuracy. The energy spectra of diatomic molecules such as I_2 and CO are examined, showing that for a fixed principal quantum number, the energy spectrum increases with increasing angular momentum quantum number, in very good agreement with previously obtained results using different analytical methods.

Keywords Stam-Cramer-Rao inequality, Schrödinger equation, Expectation values, Wave function, Information theory

Researchers have recently focused on solving both non-relativistic and relativistic equations using potential models with various analytical methods[1–5]. The derived energy equation and wave function can be applied to analyze a range of quantum mechanical systems, including the quark-antiquark system[6,7], the energy spectra of diatomic molecules (DMs)[8–10], and information theory[11–13], among others. Additionally, researchers have studied devices that coherently transfer quantum information between topological and conventional materials. In these devices, an electromagnetic field transmits a modulated signal and collects propagation channel data[14]. Shannon entropy is a key measure of the uncertainty and randomness associated with electron localization and delocalization[15]. It has recently gained prominence in quantum physics due to its crucial role in modern quantum communication systems[16]. By quantifying uncertainty in quantum systems, Shannon entropy extends Heisenberg's uncertainty principle and helps describe various physical properties[17]. In contrast, Fisher information measures the efficiency of measurement procedures and estimates quantum limits[18].

[1]Department of Physics, National Open University of Nigeria, Jabi-Abuja, Nigeria. [2]Faculty of Electronic Engineering & Technology, Universiti Malaysia Perlis, 02600 Arau, Perlis, Malaysia. [3]Centre of Excellence Advanced Communication Engineering (ACE), Universiti Malaysia Perlis, 02600 Arau, Perlis, Malaysia. [4]Group of Optoelectronic of Semiconductors and Nanomaterials, ENSAM, Mohammed V University in Rabat, 10100 Rabat, Morocco. [5]School of Electrical and Electronic Engineering, Universiti Sains Malaysia, Engineering Campus, Seberang Perai, Penang, Malaysia. ✉email: einyang@noun.edu.ng; rosdisham@unimap.edu.my

Although its theoretical basis was established earlier[19], its significance was not fully recognized until Sear et al.[20] highlighted its connection to the kinetic energy of quantum systems. Fisher information focuses on local changes in probability density[21,22] and plays an important role in fields such as density functional theory[23], statistical estimation[24], and related areas[25–34]. Shannon entropy and Fisher information are key concepts for understanding the uncertainty and precision of a system. Higher Shannon entropy indicates greater uncertainty in a system's position or momentum, with a spread-out probability distribution leading to higher entropy, while a sharply peaked distribution results in lower entropy[35]. Fisher information, on the other hand, measures the sharpness or smoothness of the probability distribution and is inversely related to uncertainty. High Fisher information suggests that small changes in position lead to significant changes in probability density, implying low uncertainty and greater system stability. This is often associated with higher kinetic energy, indicating a more localized and stable system[36]. Together, Shannon entropy and Fisher information balance uncertainty and precision in describing physical systems.

Over the past decade, research has focused on Shannon and Fisher information (FI) entropies using potential models [37,38]. For example, Dong et al. [39] extensively studied the Shannon information entropy and standard deviations of a particle in a symmetrical squared tangent potential. They illustrated the probability and entropy densities for position and momentum across different potential ranges and depths. The Bialynicki-Birula Mycielski (BBM) inequality highlights the relationship between the sum of position and momentum entropies. In another study, Song and co-workers[40] conducted a numerical investigation of Fisher information entropy in a one-dimensional system with a "Landau" potential.

The phase transition behavior of the system was effectively characterized through the development of quantum information entropy (QIE). The results show that position and momentum entropies vary with the mass parameter at the critical point of phase transition, while their total remains consistent across all excited states. Additionally, Gil-Barrera et al.[41] examined quantum information entropy in two sets of hyperbolic single potential wells. Wave functions were used to study the behavior of a moving particle under two hyperbolic potential (HP) wells. Although these hyperbolic potentials have similar shapes, their momentum entropy densities change with their widths, and position entropy density decreases as momentum entropy increases. El-Qahtani et al.[42] studied the effects of temperature on fidelity, entropy squeezing, quantum Fisher information (QFI), and two interacting superconducting qubits (SCQs). They demonstrated that the model's physical parameters can be tuned to control variations in quantum quantifiers. Additionally, they achieved a trapping phenomenon for Fisher information, which enhanced QFI, preserved the data, and protected it from temperature-induced loss. The dynamic features of quantum Fisher information in relation to the model's physical parameters were explained through the fidelity of superconducting qubits. Additionally, they explored how these physical parameters influenced the variation in superconducting qubits' squeezing entropy. Abdelmonem et al.[43] used the J-matrix method to study information entropies and related quantities for the Morse potential in both position and momentum spaces, computing the s-wave entropies of diatomic molecules H_2 and LiH numerically.

Furthermore, Edet et al.[44]. investigated quantum information using a theoretical measurement technique with Yukawa potential (YP) in curved space containing a disclination, calculating Shannon entropy based on the system's eigenfunctions. In their study, Ikot et al.[45]. applied a functional approach to derive solutions for the Schrödinger Equation (SE) involving generalized Hulthen and Yukawa potentials, using the wave function to examine information-theoretical measures in both momentum and position spaces for the ground and first excited states. Ikot et al.[46]. also analyzed Shannon and Fisher information entropies in a generalized hyperbolic potential in both position and momentum spaces by solving the SE using the NUFA method. Numerical calculations were performed to determine Shannon entropy and Fisher information entropy in both spaces. Additionally, researchers have explored modified Schrödinger Eqs[47–51].

Inspired by their methodology, we study Shannon and Fisher information entropies in one dimension and the energy spectra of selected diatomic molecules using the class of inversely quadratic Yukawa potential (CIQYP) proposed by Inyang et al.[52].

The potential is provided as:

$$V(r_q) = -\frac{d_0}{r_q} - \frac{d_1}{{r_q}^2} + \frac{d_2 e^{-\delta r_q}}{{r_q}^2} \tag{1}$$

where δ represents the screening parameter, while $d_0,\ \mathrm{d}_1,\ and\ \mathrm{d}_2$are parameters related to potential strength andr_q is the particle distance. The CIQYP could have significant applications in various fields of physics, such as atomic physics, nuclear physics, condensed matter physics, and molecular physics. This study aims to utilize normalized wave functions and energy equation to analyze information-theoretical measures in one dimension, including the expectation values of $\langle r_q \rangle$, $\left\langle {r_q}^2 \right\rangle$, $\left\langle \vec{p}^2 \right\rangle$, the energy spectra of selected diatomic molecules, and the uncertainty principle for states with low energy levels. To our knowledge, these results have not been recorded in any previously published literature.

The solutions of the Schrödinger equation with the class of inversely quadratic Yukawa potential

In this research, we use the Nikiforov-Uvarov (NU) method to solve the hypergeometric second-order differential equation. For details, refer to [53]. The radial Schrödinger equation for a quantum system with reduced mass (μ_a) is given as[54].

$$\frac{d^2R_{nl}}{dr_q{}^2}+\frac{2\mu_a}{\hbar^2}\left(E_{nl}-V\left(r_q\right)-\frac{l\left(l+1\right)\hbar^2}{2\mu_a r_q{}^2}\right)R_{nl}\left(r_q\right)=0 \tag{2}$$

To solve the radial Schrödinger equation, we insert Eq. (1) into (2) and obtain

$$\frac{d^2R_{nl}}{dr_q{}^2}+\frac{2\mu_a}{\hbar^2}\left(E_{nl}+\frac{d_0}{r_q}+\frac{d_1}{r_q{}^2}-\frac{d_2e^{-\delta r_q}}{r_q{}^2}-\frac{l\left(l+1\right)\hbar^2}{2\mu_a r_q{}^2}\right)R_{nl}\left(r_q\right)=0, \tag{3}$$

The inserted potential model cannot be solved exactly in Eq. (3). To handle the centrifugal barrier, the Greene-Aldrich approximation scheme,$r_q{}^{-2}\approx\delta^2\left(1-e^{-\delta r_q}\right)^{-2}; r_q{}^{-1}\approx\delta\left(1-e^{-\delta r_q}\right)^{-1}$ is used. This method approximates the centrifugal term well for $\delta<<1$,[55]. The change of variable $r_q\rightarrow x_c$ gives us $x_c=e^{-\delta r_q}$ as our new coordinate. With this, we can solve Eq. (3) and get

$$\frac{d^2R_{nl}\left(x_c\right)}{dx_c{}^2}+\frac{1-x_c}{x_c\left(1-x_c\right)}\frac{dR\left(x_c\right)}{dx_c}+\frac{1}{\left[x_c\left(1-x_c\right)\right]^2}\left[-\varepsilon x_c{}^2+\left(2\varepsilon-\beta_x-\beta_z\right)x_c-\left(\varepsilon-\beta_x-\beta_y+\gamma_a\right)\right]R\left(x_c\right)=0, \tag{4}$$

where

$$-\varepsilon=\frac{2\mu_aE_{nl}}{\delta^2\hbar^2},\beta_x=\frac{2\mu_ad_0}{\delta\hbar^2},\beta_y=\frac{2\mu_ad_2}{\hbar^2},\beta_z=\frac{2\mu_ad_1}{\hbar^2},\gamma_a=l\left(l+1\right)\Big\}. \tag{5}$$

Comparing Eqs. (4) and (1) of Ref. [53] yields the following polynomials:

$$\begin{aligned}\widetilde{\tau}\left(x_c\right)&=1-x_c;\sigma\left(x_c\right)=x_c\left(1-x_c\right);\sigma^{/}\left(x_c\right)=1-2x_c,\\ \widetilde{\sigma}\left(x_c\right)&=-\varepsilon x_c{}^2+\left(2\varepsilon-\beta_x-\beta_z\right)x_c-\left(\varepsilon-\beta_x-\beta_y+\gamma_a\right)\end{aligned}. \tag{6}$$

Putting the polynomials in Ref. [53] of Eq. (11) gives the polynomial

$$\pi\ \left(x_c\right)=-\frac{x_c}{2}\ \pm\sqrt{\left(\Upsilon_1-K_s\right)x_c{}^2+\left(K_s+\Upsilon_2\right)x_c\ +\ \Upsilon_3}, \tag{7}$$

where

$$\Upsilon_1=\left(\frac{1}{4}+\varepsilon\right),\Upsilon_2=-\left(2\varepsilon-\beta_x-\beta_z\right),\Upsilon_3=\left(\varepsilon-\beta_x-\beta_y+\gamma_a\right) \tag{8}$$

The NU method states that the discriminant of this quadratic equation (QE) is set to zero. The discriminant provides a new QE that can be solved to find the two roots for the constant . Here, we consider the negative square root provided as

$$K_s=-\left(\Upsilon_2+2\Upsilon_3\right)-2\sqrt{\Upsilon_3}\sqrt{\Upsilon_3+\Upsilon_2+\Upsilon_1}. \tag{9}$$

We then put K_s into $\pi\ \left(x_c\right)=-\frac{x_c}{2}\ \pm\sqrt{\left(\Upsilon_1-K_s\right)x_c{}^2+\left(K_s+\Upsilon_2\right)x_c\ +\ \Upsilon_3}$, and obtain, $\pi\left(x_c\right)$has the most suitable expression given as

$$\pi\left(x_c\right)=-\frac{x_c}{2}-\left[\left(\sqrt{\Upsilon_3}+\sqrt{\Upsilon_3+\Upsilon_2+\Upsilon_1}\right)x_c-\sqrt{\Upsilon_3}\right], \tag{10}$$

Utilizing the polynomials and Eq. (10). Hence, we deduce $\tau\left(x_c\right)$ and $\tau^{/}\left(x_c\right)$ in the following manner:

$$\tau\left(x_c\right)=1-2x_c-2\sqrt{\Upsilon_3}x_c-2\sqrt{\Upsilon_3+\Upsilon_2+\Upsilon_1}x_c+2\sqrt{\Upsilon_3}, \tag{11}$$

$$\tau^{/}\left(x_c\right)=-2\left[1+\sqrt{\Upsilon_3}+\sqrt{\Upsilon_3+\Upsilon_2+\Upsilon_1}\right]. \tag{12}$$

The expressions for $\lambda_{.n}$ and λ can be found in Eq. (10) and Eq. (13) of Reference [53].

$$\lambda_{.n}=n^2+\left[1+2\sqrt{\Upsilon_3}+2\sqrt{\Upsilon_3+\Upsilon_2+\Upsilon_1}\right]n, \tag{13}$$

$$\lambda=-\frac{1}{2}-\sqrt{\Upsilon_3}-\sqrt{\Upsilon_3+\Upsilon_2+\Upsilon_1}-\left(\Upsilon_2+2\Upsilon_3\right)-2\sqrt{\Upsilon_3}\sqrt{\Upsilon_3+\Upsilon_2+\Upsilon_1}, \tag{14}$$

Equating Eqs. (13) and (14), and substituting Eq. (5), the energy eigenvalues of the SE for CIQYP are obtained.

$$E_{nl} = \frac{\delta^2\hbar^2 l\,(l+1)}{2\mu_a} - d_2\delta^2 - d_0\delta - \frac{\delta^2\hbar^2}{8\mu_a}\left[\begin{array}{l}\left(n+\frac{1}{2}+\sqrt{\left(l+\frac{1}{2}\right)^2+\frac{2\mu_a d_2}{\hbar^2}-\frac{2\mu_a d_1}{\hbar^2}}\right)^2 \\ \frac{-\frac{2\mu_a d_0}{\delta\hbar^2}-\frac{4\mu_a d_2}{\hbar^2}+\frac{2\mu_a d_1}{\hbar^2}+l\,(l+1)}{n+\frac{1}{2}+\sqrt{\left(l+\frac{1}{2}\right)^2+\frac{2\mu_a d_2}{\hbar^2}-\frac{2\mu_a d_1}{\hbar^2}}}\end{array}\right]^2. \tag{15}$$

The wave function is obtained as

$$R_{nl}(x_c) = N_{nl}x_c^{\sqrt{\Upsilon_3}}(1-x_c)^{\frac{1}{2}+\sqrt{\Upsilon_1+\Upsilon_2+\Upsilon_3}} \times P_n^{\left(2\sqrt{\Upsilon_1},2\sqrt{\Upsilon_1+\Upsilon_2+\Upsilon_3}\right)}(1-2x_c) \tag{16}$$

Let $S_1 = \sqrt{\Upsilon_3}$

$S_2 = \sqrt{\Upsilon_1+\Upsilon_2+\Upsilon_3}$

$R_{nl}(x_c) = N_{nl}x_c^{S_1}(1-x_c)^{\frac{1}{2}+S_2} \times P_n^{(2S_1,2S_2)}(1-2x_c)$

$$x_c = e^{-\delta r_q} \tag{17}$$

The normalization constant condition is:

$$\int_0^\infty R_{nl}(r_q)R_{nl}^*(r_q)dr_q = 1 \tag{18}$$

Utilizing the wave function

$$N_{nl}^2\int_0^\infty dr_q\left(e^{-\delta r_q}\right)^{2S_1}\left(1-e^{-\delta r_q}\right)^{2S_2+1}\left[P_n^{(2S_1,2S_2)}\left(1-2e^{-\delta r_q}\right)\right]^2 \tag{19}$$

$x_c = e^{-\delta r_q} \in (1,0)$

Let $dx_c = -\delta x_c dr_q$

$dr_q = -\frac{dx_c}{\delta x_c}$

By changing variable of Eq. (19) We have,

$$\frac{N_{nl}^2}{\delta}\int_0^1 x_c^{2S_1-1}(1-x_c)^{2S_2+1} \times \left[P_n^{(2S_1,2S_2)}(1-2x_c)\right]^2 dx_c \tag{20}$$

The Jacobi function $P_n^{(2S_1,2S_2)}(1-2x_c)$ given in Refs[56,57] can be expressed respectively as

$$\begin{aligned}P_n^{(2S_1,2S_2)}(1-2x_c) &= (-1)^n\Gamma(n+2S_1+1)\,\Gamma(n+2S_2+1)\\ &\times\sum_{j=0}^{n}\frac{(-1)^j x_c^{n-j}(1-x_c)^j}{j!\,(n-j)!\Gamma(n+2S_1-j+1)} \times \Gamma(2S_2+j+1)\end{aligned} \tag{21}$$

$$P_n^{(2S_1,2S_2)}(1-2x_c) = \frac{\Gamma(n+2S_2+1)}{\Gamma(n+2S_2+2S_1+1)} \times \sum_{k=0}^{n}\frac{(-1)^k\Gamma(n+2S_2+2S_1+k+1)\,x_c^k}{k!\,(n-k)!\Gamma(2S_1+k+1)} \tag{22}$$

Substituting Eqs. (21) and (22) into Eq. (20) yields

$$\begin{aligned}&(-1)^n\frac{\Gamma[n+2S_1+1]^2\Gamma(n+2S_2+1)}{\Gamma(2S_1+2S_2+n+1)}\\ &\times\sum_{j=0}^{n}\sum_{k=0}^{n}\frac{(-j)^{j+k}\Gamma(n+2S_1+2S_2+k+1)\times I_{nl}(j.k)}{j!\,(n-j)!k!\,(n-k)!\Gamma(n+2S_1-j-1)\times\Gamma(2S_1+k+1)}\end{aligned} \tag{23}$$

where

$$I_{nl}\left(j,k\right)=\frac{N_{nl}^{2}}{\delta}\int_{0}^{1}x_{c}^{2S_{1}+n+k-j-1}(1-x_{c})^{2S_{2}+j+1}dx_{c} \tag{24}$$

Equation 24 can be written in a conventional format as described in references[56,57].

$$\int_{0}^{1}x_{c}^{t-1}(1-x_{c})^{-h}dx_{c}=\frac{2F_{1}\left(t,h:t+1:1\right)}{t} \tag{25}$$

The Hypergeometric function is defined as

$$2F_{1}\left(t,h:t+1:1\right)=\frac{\Gamma(t+1)\Gamma(1-h)}{\Gamma(t-h+1)} \tag{26}$$

Using (24) and (25), one obtains

$$I_{nl}(j,k)=\frac{\Gamma\left(n+2S_{1}+k-j\right)\left(2S_{2}+j+1\right)\Gamma\left(2S_{2}+j+1\right)}{\left(n+2S_{1}+2S_{2}+k+1\right)\Gamma\left(n+2S_{1}+2S_{2}+k+1\right)}\times\frac{N_{nl}^{2}}{\delta} \tag{27}$$

Substituting (27) into (23).

The normalization constant is obtained as

$$N_{nl}=\frac{1}{\sqrt{L_{nl}}} \tag{28}$$

where

$$\begin{aligned}L_{nl}&=\frac{\left(\Gamma\left(2S_{1}+n+1\right)\right)^{2}\Gamma\left(n+2S_{2}+1\right)}{\delta\Gamma\left(n+2S_{1}+2S_{2}+1\right)}(-1)^{n}\\&\times\sum_{j=0}^{n}\sum_{k=0}^{n}\frac{(-1)^{j+k}\Gamma\left(n+2S_{1}+k-j\right)\left(2S_{2}+j+1\right)}{j!(n-j)!k!(n-k)!\Gamma(n+2S_{1}-j+1)\Gamma(2S_{1}+k+1)}\times\left(2S_{1}+2S_{2}+n+k+1\right)\end{aligned} \tag{29}$$

The Fourier transform is used to derive the momentum WF in one dimension.

$$R_{nl}(p)=\frac{1}{\sqrt{2\pi}}\int_{0}^{\infty}R_{nl}(r_{q})e^{-ipr_{q}}dr_{q} \tag{30}$$

Using the explicit notation for the Jacobi function (22), Eq. (30) reduces to

$$\begin{aligned}R_{nl}(p)&=\frac{N_{nl}}{\sqrt{2\pi}}\frac{\Gamma\left(2S_{1}+n+1\right)}{\Gamma\left(2S_{1}+2S_{2}+n+1\right)}\\&\times\sum_{k=0}^{n}\frac{(-1)^{k}\Gamma\left(n+2S_{1}+2S_{2}+k+1\right)}{k!(n-k)!\Gamma(2S_{1}+k+1)}\times\int_{0}^{\infty}\left(e^{-\delta r_{q}}\right)^{2S_{1}+k}\left(1-e^{-\delta r_{q}}\right)^{2S_{2}+\frac{1}{2}}e^{-ipr_{q}}dr_{q}\end{aligned} \tag{31}$$

The Mathematica 13 software yields the value of $R_{nl}(p)$as

$$\begin{aligned}R_{nl}(p)&=\frac{N_{nl}}{\sqrt{2\pi}}\times\frac{\Gamma\left(n+2S_{1}+1\right)\Gamma\left(S_{2}+\frac{3}{2}\right)\Gamma\left(S_{1}+\frac{ip}{\delta}\right)}{\phi_{a}\Gamma\left(2S_{1}+1\right)n!\Gamma\left(S_{1}+S_{2}+\frac{3}{2}+\frac{ip}{\delta}\right)}\\&\times PF_{q}\left[\left(-n,n+2S_{1}+2S_{2}+1,S_{1}+\frac{ip}{\delta}\right),\left(2S_{1}+1,S_{1}+S_{2}+\frac{3}{2}+\frac{ip}{\delta}\right),1\right]\end{aligned} \tag{32}$$

Mathematica 13 allows users to input equations and expressions in symbolic form. It performs symbolic manipulation, numerical computation, and optimization using Wolfram Language programming.

Expectation values of position (r_q), position square($r_q{}^2$), and momentum square($\hat{p}^2$) ofr_q, $r_q{}^2$and $\vec{p}^2$for the CIQYP and the Heisenberg Uncertainty principle

Expectation value for position

The expression provides the expectation value (EV) of position (r_q) as follows [58].

$$\langle r_q \rangle_n = \int_0^\infty R_{n\ell}\, r_q\, R_{.n\ell} dr_q \tag{33}$$

Expectation value for position square

The expression provides the expectation value of position square ($r_q{}^2$)as follows [58].

$$\left\langle r_q{}^2 \right\rangle_n = \int_0^\infty R_{.n\ell}\, r_q{}^2\, R_{n\ell} dr_q \tag{34}$$

Expectation value of momentum square

Similarly, the expectation value of momentum square ($\hat{p}^2$)is represented as [58].

$$\left\langle \hat{p}^2 \right\rangle_n = \int_0^\infty R_{n\ell}\, \hat{p}^2\, R_{.n\ell} dr_q = \quad -\int_0^\infty R_{nl}\,(r)\,\hbar^2\,\frac{d^2}{dr_q^2} R^*_{n.l}\,(r)\,dr_q \tag{35}$$

The one-dimensional average momentum value $\left\langle p^2 \right\rangle$ can also be calculated using integral relationships.

$$\left\langle p^2 \right\rangle = \int_{-\infty}^\infty R_{nl}\,(p)\, p^2\; R^*_{nl}\,(p)\, dp \tag{36}$$

It is essential to confirm that Eqs. (35) and (36) are equal and in one dimension the expectation value would be zero as a result of symmetry.

Heisenberg Uncertainty

When assessing ground state uncertainty, the uncertainties of position and momentum are evaluated in the following manner:

Uncertainty in position
Applying the relation [58];

$$\Delta r_q = \sqrt{\langle r_q^2 \rangle - \langle r_q^2 \rangle} \tag{37}$$

Uncertainty in momentum
Applying the relation [58];

$$\Delta p = \sqrt{\langle p^2 \rangle - \langle p^2 \rangle} \tag{38}$$

Using the Wolfram Mathematica 13 software program, the expectation values for $r_q, r_q{}^2, \vec{p}^2$ will be determined, along with the associated uncertainties.

The Shannon entropy

Shannon entropy measures the degree of randomness and unpredictability in a particle's spatial location through a logarithmic function. Reference[59] contains the Shannon entropy calculated in both position and momentum spaces.

$$S_{r_q} = -\int_0^\infty \rho(r_q) In\rho(r_q) dr_q \tag{39}$$

and

$$S_p = -\int_0^\infty \rho(p) In\rho(p) dp \tag{40}$$

where S_{r_q} represents the Shannon entropy in position space, while S_p represents the Shannon entropy in momentum space.

Position and momentum space probability densities (PD) are, $\rho(r_q) = |\psi(r_q)|^2$ and $\rho(p) = |R(p)|^2$ respectively. The BBM suggested Shannon entropic uncertainty relation has$S_T = S_{r_q} + S_p \geqslant D[1 + (\mathrm{In}\pi)]$, where D is the spatial dimension[60]. All quantum states normalized wave function in momentum space is calculated using the Fourier transform[61].

$$R(p) = \frac{1}{\sqrt{2\pi}} \int_0^\infty \psi(r_q) e^{-ipr_q} dr_q \tag{41}$$

The Fisher information

In position and momentum spaces, Fisher information focuses on local probability.

distribution changes. Density functional is essential for studying Fisher information[62]. As stated in reference[63],

$$I_{r_q} = \int \frac{|\rho'(r_q)|^2}{\rho(r_q)} dr_q = 4 \int \left|\psi'(r_q)\right|^2 dr_q = 4\langle p^2\rangle - 2(2l+1)|m|\langle r_q^{-2}\rangle \tag{42}$$

$$I_p = \int \frac{|\rho'(p)|^2}{\rho(p)} dp = 4 \int \left|\psi'(p)\right|^2 dp = 4\langle r_b^2\rangle - 2(2l+1)|m|\langle p^{-2}\rangle \tag{43}$$

We use Mathematica 13 software to solve Eqs. (42) and (43) because they are difficult to solve analytically due to the integral's complex form.

Application to diatomic molecules

Diatomic molecules, consisting of just two atoms bonded together, are fundamental building blocks in physics and chemistry. They are essential to everything in our world, from the materials we use to the air we breathe. Recent studies by authors[64–68] have explored these molecules in greater detail. Our adopted potential can be used to investigate diatomic molecules through setting $d_0 = 2D_e r_e, d_1 = -D_e r_e^2, d_2 = 0$of Eq. (1), we have the Kratzer potential[69] and the energy equation is given as Eq. (44),when $\delta = 0$. The Kratzer potential has become increasingly significant in atomic and molecular physics, as well as in vibrational and rotational spectroscopy[70]. Its importance in molecular physics is substantial and widely recognized.

$$E_{nl} = -\frac{2\mu_a}{\hbar^2} D_e^2 r_e^2 \left[n + \frac{1}{2} + \sqrt{\left(l + \frac{1}{2}\right)^2 + \frac{2\mu_a D_e r_e^2}{\hbar^2}} \right]^{-2} \tag{44}$$

Results and discussion

The NU method is used to determine the Schrödinger equation eigenstates with the CIQYP in closed form. For any principal quantum number (PQN), the wave function is normalized using the normalization condition and orthogonal functions, such as Jacobi and hypergeometric functions. The one-dimensional Fourier transform is applied to obtain the momentum space wave function. We then analyze Shannon and Fisher information entropies in both position and momentum spaces, along with the expectation values of $\langle r_q\rangle$, $\langle {r_q}^2\rangle$, $\langle \vec{p}^2\rangle$, and uncertainty relations to assess the localization of a quantum mechanical system.

Tables 1 and 2 demonstrate that as the screening parameter (SP) increases, the Shannon entropy in momentum space decreases for the ground and first excited states, while the Shannon entropy in position space increases. This adjustment ensures that the sum meets the BBM inequality, which requires that the lower bound of Shannon entropy be greater than or equal to $(1+\ln(\pi))$. Shannon entropy measures the overall uncertainty or disorder in a system, reflecting how spread out its possible states are. As the screening parameter increases for the ground and first excited states, Fisher information in position space increases, while Fisher entropies in momentum space decrease, thereby satisfies the inequality relations$I_{r_b} I_p \geq 4$. Fisher information is related to the kinetic energy of a system, where higher Fisher information typically indicates higher kinetic energy. This suggests that the system is more localized and less uncertain, contributing to greater stability. Conversely, lower Fisher information implies a more diffuse state, potentially leading to lower stability. By exploring the interplay between position and momentum Fisher entropies, this study sheds light on a fundamental aspect of the Heisenberg uncertainty principle, which emphasizes the inherent limitations in simultaneously measuring certain conjugate variables (such as position and momentum) with absolute precision. Fisher information measures the sensitivity or precision of a system, indicating how much information can be extracted from small changes. Both entropies are crucial for balancing uncertainty and precision in describing physical systems. Numerical calculations for various expectation values at the ground and first excited states are presented in Table 2, showing a more concentrated distribution for smaller values of the screening parameter. The product of the uncertainties in position and momentum for these states validates the Heisenberg uncertainty relation (HUR)[71–75]. The HUR asserts that as uncertainty in position increases, uncertainty in momentum decreases, and vice versa. Our results confirm this behavior. The potential model was simplified to the Kratzer potential using specific boundary conditions, ensuring the mathematical precision of our analytical calculations. Spectroscopic

$n_{=0}$	δ	S_{r_q}	S_p	$S_T \geq 2.14473$
	0.01	−0.285132	2.491861	2.206729
	0.02	0.0755000	2.132443	2.887443
	0.03	0.2892130	1.917739	2.206952
	0.04	0.4444960	1.762474	2.206970
	0.05	0.5671890	1.639808	2.206997
	0.06	0.6254311	1.576345	2.201776
	0.07	0.7342100	1.467320	2.201530
	0.10	0.9704820	1.368850	2.273670
n = 1	0.01	0.1894810	2.695827	2.885308
	0.02	0.5524940	2.332825	2.885319
	0.03	0.7703690	2.114981	2.885350
	0.04	0.9285480	1.956865	2.885413
	0.05	1.0539950	1.831525	2.885520
	0.06	1.2541010	1.732647	2.986748
	0.07	1.3152080	1.693356	3.008564
	0.10	1.4728750	1.414263	2.887138

Table 1. The ground and first excited states of the Shannon entropy values for CIQYP.

n = 0	δ	I_{r_b}	I_p	$I_{r_b} I_p \geq 4$	$\langle r_b^2 \rangle$	r_q	$\langle p^2 \rangle$	$\Delta p \Delta r_q \geq 0.50$
	0.01	34.71861	0.120755	4.192445	0.421263	0.621311	8.679500	0.553021
	0.02	16.91987	0.247887	4.194215	0.864441	0.890019	4.229689	0.553024
	0.03	11.01348	0.380673	4.192534	1.328041	1.103154	2.753094	0.553033
	0.04	8.072889	0.519415	4.193179	1.811529	1.288400	2.018198	0.553051
	0.05	6.317723	0.664826	4.200186	2.314971	1.456455	1.579153	0.553082
	0.06	5.533879	0.765438	4.235839	2.456363	1.623410	1.324510	0.553145
	0.07	4.765202	0.887462	4.317681	3.564321	1.834215	1.108945	0.553189
	0.10	2.422903	1.849996	4.482361	5.172624	2.176789	0.705726	0.553566
n = 1	0.01	54.83589	0.141302	7.748420	1.123415	0.999211	13.93149	1.319596
	0.02	26.96296	0.269361	7.262769	2.321883	1.436505	6.740463	1.319584
	0.03	17.43840	0.417279	7.276678	3.589722	1.786148	4.359600	1.319550
	0.04	12.71918	0.570792	7.260006	4.924980	2.092132	3.177295	1.319483
	0.05	9.799187	0.732765	7.180501	6.328248	2.371530	2.472297	1.319367
	0.06	7.787354	0.877995	7.022514	7.432567	2.598345	2.109845	1.319235
	0.07	6.008098	0.932146	6.899746	9.875432	2.754327	1.845624	1.317986
	0.10	3.278714	1.864930	6.114572	14.58355	3.600116	1.069679	1.317489

Table 2. Expectation values of $\langle r_q \rangle$, $\langle r_q^2 \rangle$, $\langle \bar{p}^2 \rangle$,Fisher Information entropy, and the uncertainty relation for the ground and first excited states for the CIQYP.

Molecules	$D_e\ (eV)$	$r_e\ (\mathring{A})$	$\mu\ (amu)$
CO	10.84514471	1.1282	6.860586000
I_2	1.581791863	2.6620	63.45223502

Table 3. Spectroscopic parameters of the selected diatomic molecules [76] .

data for these molecules, sourced from reference[76], are presented in Table 3. The calculations were performed using the conversions outlined by 1 amu=931.494028 MeV/c^2 and ħ=1973.29 eV Å[77]. The selection of these diatomic molecules was based on extensive applications and studies conducted by various researchers. We calculate the energy eigenvalues using Eq. (44) and the parameters given in Table 3 for CO and I_2 diatomic molecules. The energy eigenvalues are presented in Table 4 for different n and l quantum numbers and are in good agreement with results obtained previously using different analytical methods [76,78]. It was observed that for constant n and varying l, the energy increases. This implies that, for a quantum system such as an atom, increasing the orbital angular momentum quantum number (l) at a constant principal quantum number (n)

n	l	I_2	I_2[76]	CO	CO[76]
0	0	− 1.5790825	− 1.579082577	− 10.794315	− 10.79431532
1	0	− 1.5736871	− 1.573687151	− 10.693839	− 10.69383992
	1	− 1.5736779	− 1.573677925	− 10.693371	− 10.69337123
2	0	− 1.5683193	− 1.568319330	− 10.594760	− 10.59476089
	1	− 1.5683101	− 1.568310152	− 10.594298	− 10.59429869
	2	− 1.5682917	− 1.568291796	− 10.593374	− 10.59337441
3	0	− 1.5629789	− 1.562978927	− 10.497052	− 10.49705246
	1	− 1.5629697	− 1.562969796	− 10.496596	− 10.49659664
	2	− 1.5629515	− 1.562951533	− 10.495685	− 10.49568512
	3	− 1.5629241	− 1.562924140	− 10.494318	− 10.49431814
4	0	− 1.5576657	− 1.557665755	− 10.400689	− 10.40068947
	1	− 1.5576566	− 1.557656670	− 10.400239	− 10.40023992
	2	− 1.5576385	− 1.557638501	− 10.399340	− 10.39934092
	3	− 1.5576112	− 1.557611248	− 10.397992	− 10.39799272
	4	− 1.5575749	− 1.557574911	− 10.396195	− 10.39619567
5	0	− 1.5523796	− 1.552379630	− 10.305647	− 10.30564735
	1	− 1.5523705	− 1.552370591	− 10.305203	− 10.30520394
	2	− 1.5523525	− 1.552352514	− 10.304317	− 10.30431723
	3	− 1.5523253	− 1.552325399	− 10.302987	− 10.30298747
	4	− 1.5522892	− 1.552289247	− 10.301214	− 10.30121499
	5	− 1.5522440	− 1.552244060	− 10.299000	− 10.29900024

Table 4. Comparison of the bound state Energy (in eV) for the various n and l quantum numbers for a few diatomic molecules at constant n.

Molecule	$\alpha\left(\overset{0}{\mathrm{A}}\right)^{-1}$	μ (amu)
N_2	2.69860	7.0033500000
O_2	1.295515	7.9974575040
NO	2.75340	7.4684410000

Table 5. Spectroscopic parameters of the molecules used in this work [81].

leads to higher bound state energy. Higher l values correspond to higher centrifugal barriers, which reduce the effective potential well depth experienced by the particle. As a result, the particle is less tightly bound, leading to higher energy states. In Table 5, we numerically present the eigenvalues of the CIQYP for three diatomic molecules (N_2, O_2, and NO) using the energy equation given in Eq. (15). This was done by inputting the model parameters for each molecule[79], as shown in Table 6. The results indicate that the bound state energy spectra of these diatomic molecules increase as the various quantum numbers n and l increase. Figure 1a,b display the behavior of the wave function and probability density in position space for various principal quantum numbers, with angular momenta equal to 1 and 2. Figure 1a shows that as the principal quantum number increases, the wave function exhibits a corresponding increase. Figure 1b illustrates how the wave function changes with different potential parameters to meet the BBM conditions. The wave functions display multiple sinusoidal curves representing various quantum states, which intertwine with each other while all other parameters remain constant. The BBM inequality implies a trade-off between the uncertainties in different properties of a system, such as position and momentum. It sets a lower bound on these uncertainties, meaning that as one property becomes more precisely known, the uncertainty in the other increases, and reflecting inherent limitations in the system's precision. Figure 2a, b depict the graphs of the probability density function for $l=1$ and $l=2$. The probability density plots show normal distribution curves with multiple peaks, each representing a distinct quantum state. Figure 2a indicates higher accuracy in predicting particle localization and greater stability in the quantum system. Figure 2(b) displays a probability density with comparable patterns, suggesting that the probability densities for these entropies are concentrated in specific regions. Under ideal conditions, the peak of the probability density plot is expected to rise with an increase in the quantum state, and the wave function typically becomes more complex, with more nodes or oscillations. The plot of the momentum space probability density for $n=0$ with different potential parameters as a function of p is depicted in Fig. 3. The probability density plot follows a spectrally Gaussian distribution, exhibiting quantized curves with varying peaks depending on the optimization parameter. Sinusoidal wave functions representing different quantum states highlight position and momentum uncertainty, consistent with the Heisenberg Uncertainty Principle. Increased uncertainty raises Shannon entropy, while reduced clarity in quantum states lowers Fisher information, demonstrating the trade-off

n		N_2	O_2	NO
0	0	−2.932142	−1.535081	−2.987606
1	0	−2.882584	−1.508025	−2.938646
	1	−2.880808	−1.507290	−2.936923
2	0	−2.839697	−1.483071	−2.896155
	1	−2.838125	−1.482391	−2.894625
	2	−2.834998	−1.481037	−2.891582
3	0	−2.803121	−1.460106	−2.859798
	1	−2.801742	−1.459479	−2.858451
	2	−2.799003	−1.458230	−2.855772
	3	−2.794939	−1.456367	−2.851796
4	0	−2.772524	−1.439024	−2.829262
	1	−2.771330	−1.438448	−2.828089
	2	−2.768958	−1.437299	−2.825758
	3	−2.765443	−1.435586	−2.822300
	4	−2.760837	−1.433321	−2.817763
5	0	−2.747603	−1.419728	−2.804259
	1	−2.746584	−1.419199	−2.803252
	2	−2.744562	−1.418146	−2.801251
	3	−2.741570	−1.416576	−2.798289
	4	−2.737656	−1.414500	−2.794408
	5	−2.732885	−1.411936	−2.789668

Table 6. Energy spectra (in eV) of the class of inversely quadratic potential for

between uncertainty and information in the system.The characteristics of the position and momentum densities align with previous research on one-dimensional systems with various potential functions, as documented in the literature[80,81].

Conclusions

In this research, we solve the Schrödinger equation with the CIQYP using the NU technique. With the derived energy equation and normalized wave function, we examine the expectation values of $\langle r_q \rangle$, $\langle {r_q}^2 \rangle \langle \vec{p}^2 \rangle$, as well as the Shannon entropy and Fisher information for position and momentum spaces. The information theory measures, including Shannon entropy and Fisher information, provide an alternate uncertainty relation. A physical system must satisfy the BBM and Stam-Cramer-Rao (SCR) inequalities to be considered physically stable. Our results, as shown in the tables, satisfy the BBM and SCR inequalities, and we theoretically prove that the Heisenberg uncertainty principle is also satisfied. The eigenvalues of the CIQYP for three diatomic molecules (N_2, O_2, and NO) are numerically presented, showing that the bound state energy spectra of these diatomic molecules increase as various quantum numbers increase. Additionally, our potential model was simplified to the Kratzer potential through the application of specific boundary conditions, ensuring the mathematical precision of our analytical calculations. The energy eigenvalues obtained for the CO and I_2 diatomic molecules are in excellent agreement with previously obtained results using different analytical methods.

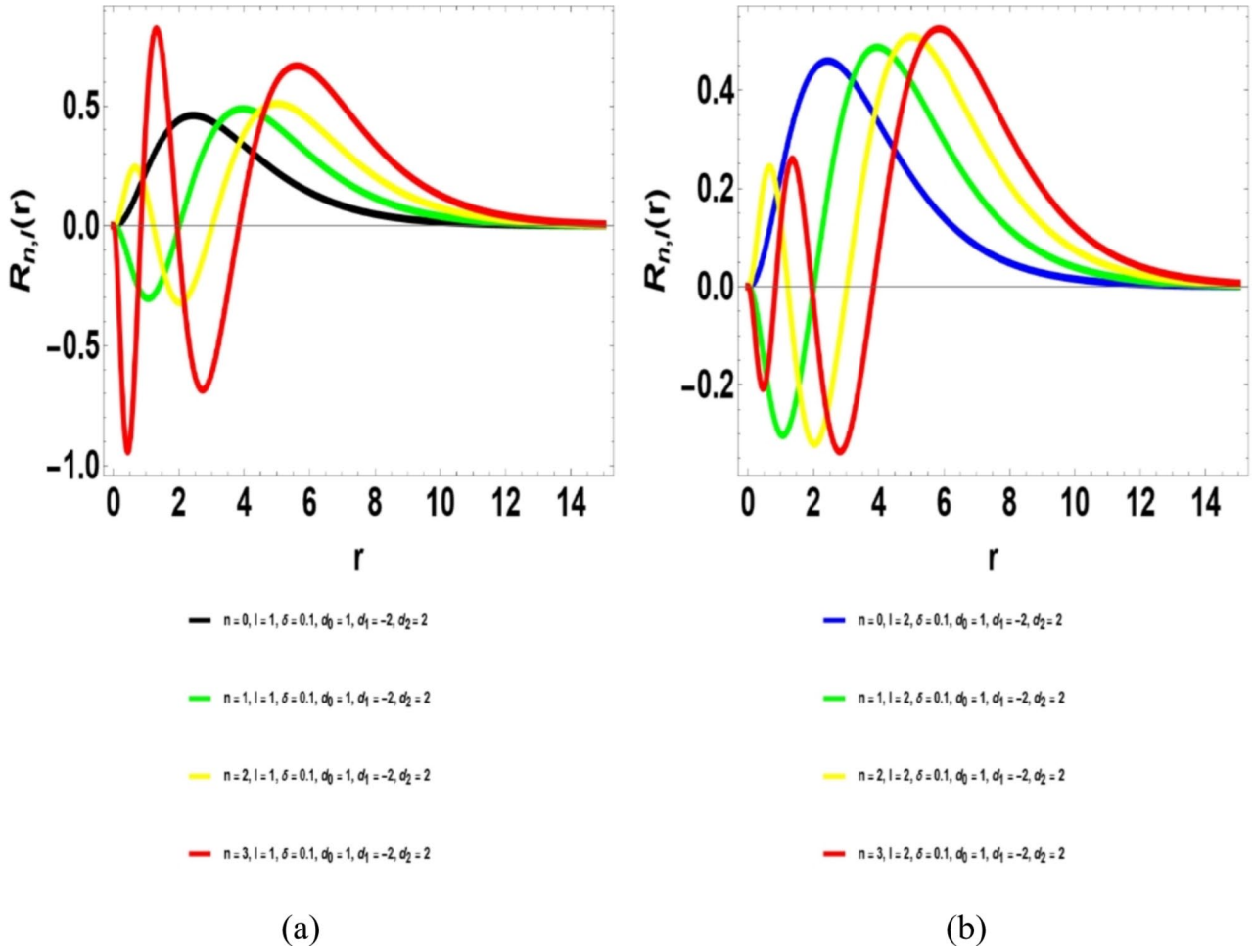

Fig. 1. (**a**, **b**): The class of inversely quadratic Yukawa potential wave function as a function of position for various principal quantum numbers at l =1 and l =2.

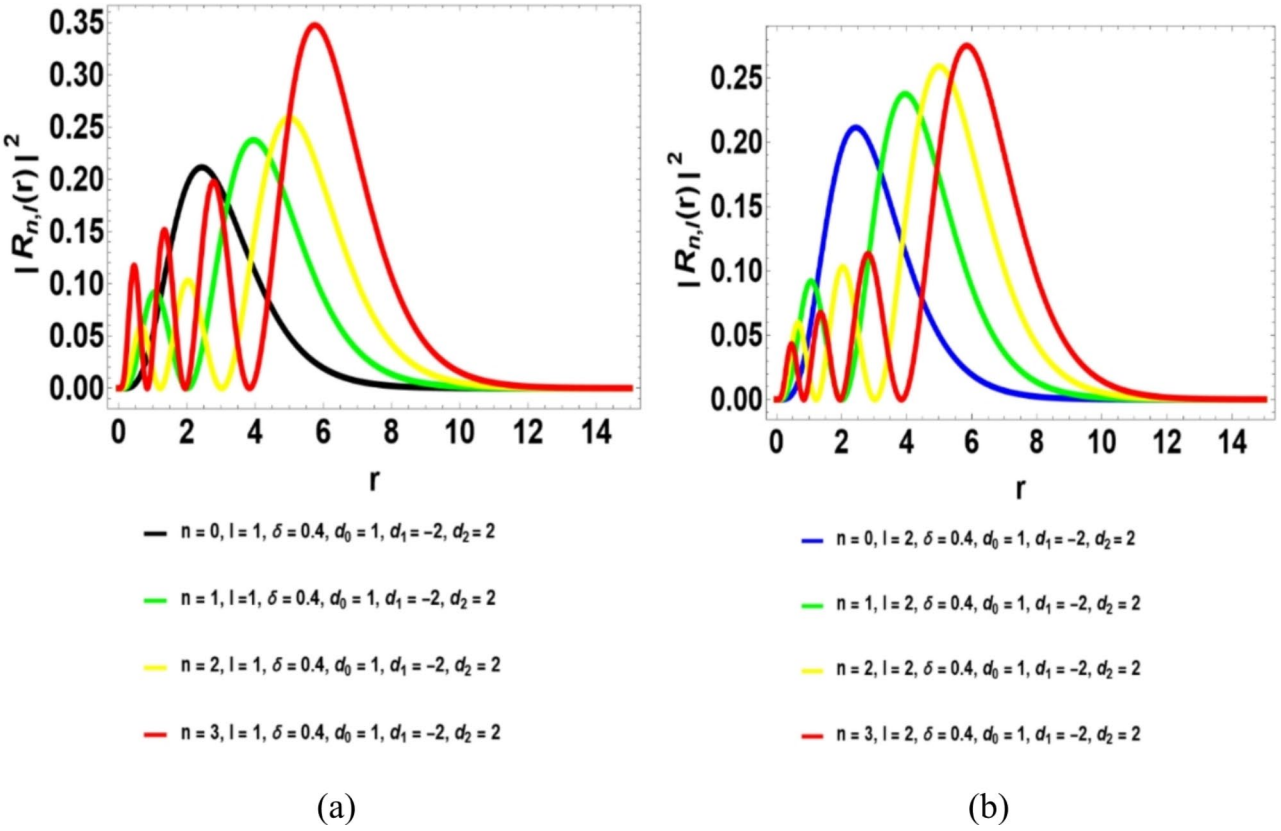

Fig. 2. (**a**, **b**): The probability density of the class of inversely quadratic Yukawa potential at $l = 1$ and $l = 2$ as a function of position for various principal quantum numbers.

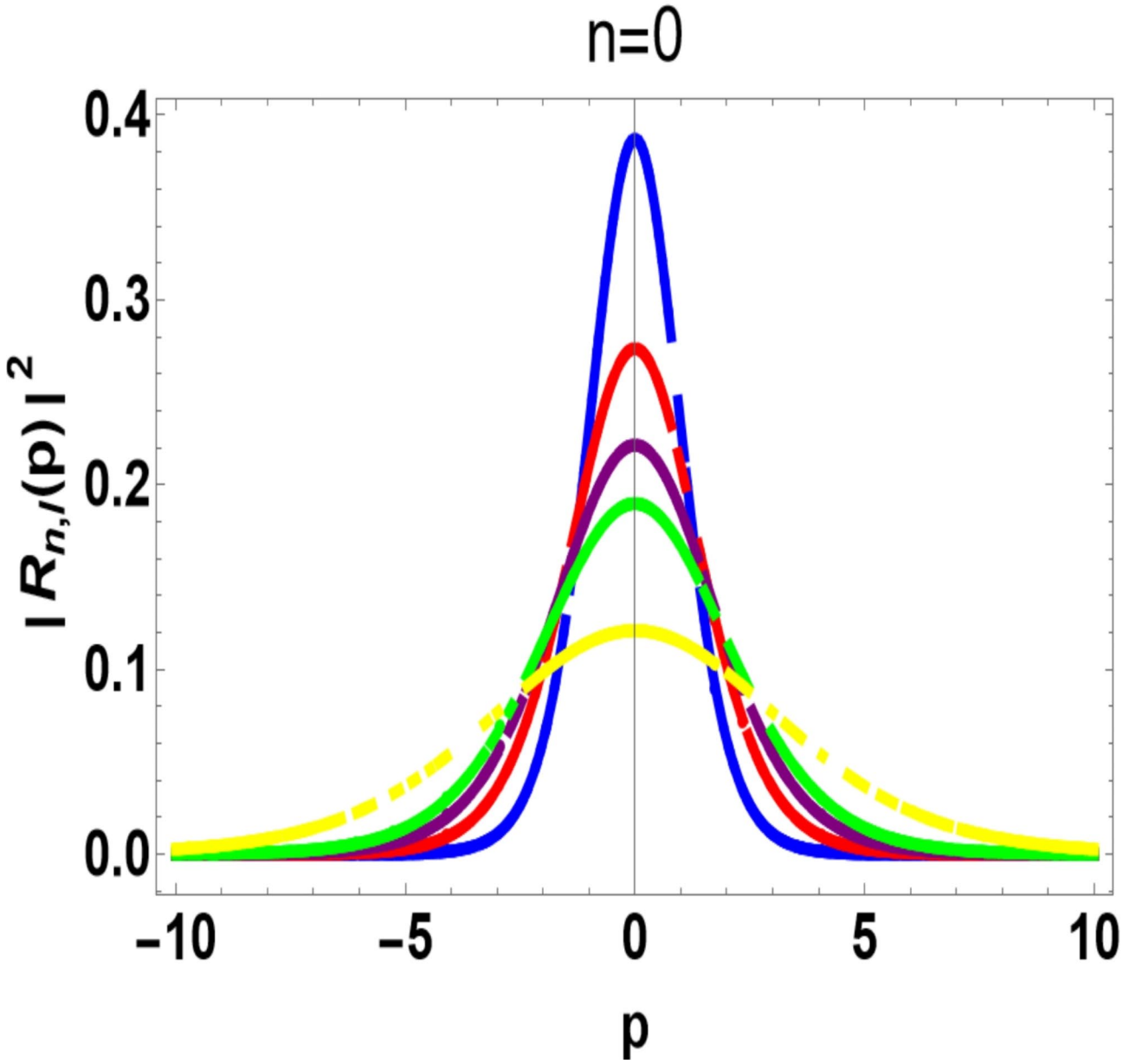

Fig. 3. Momentum space probability density plot for $n = 0$.

Data availability

All data generated or analysed during this study are included in this published article.

Appendix A: review of Nikiforov-Uvarov (NU) method

The NU method was proposed by Nikiforov and Uvarov [53] to transform Schrödinger-like equations into a second-order differential equation via a coordinate transformation $x_c = x_c(r)$, of the form

$$\psi''(x_c) + \frac{\tilde{\tau}(x_c)}{\sigma(x_c)}\psi'(s) + \frac{\tilde{\sigma}(x_c)}{\sigma^2(x_c)}\psi(x_c) = 0 \tag{A1}$$

where $\tilde{\sigma}(x_c)$, and $\sigma(x_c)$ are polynomials, at most second degree and $\tilde{\tau}(x_c)$ is a first-degree polynomial. The exact solution of Eq.(A1) can be obtain by using the transformation.

$$\psi(x_c) = \phi(x_c)\, y(x_c) \tag{A2}$$

This transformation reduces Eq.(A1) into a hypergeometric-type equation of the form

$$\sigma(x_c)\,y''(x_c)+\tau(x_c)\,y'(x_c)+\lambda y(x_c)=0 \tag{A3}$$

The function$\phi(x_c)$ can be defined as the logarithm derivative

$$\frac{\phi'(x_c)}{\phi(x_c)}=\frac{\pi(x_c)}{\sigma(x_c)} \tag{A4}$$

where $\pi(x_c)$ being at most a first-degree polynomial.The second part of $\psi(x_c)$ in Eq. (A2) is the hypergeometric function with its polynomial solution given by Rodrigues relation as.

$$y(x_c)=\frac{B_{nl}}{\rho(x_c)}\frac{d^n}{dx_c{}^n}\left[\sigma^n(x_c)\,\rho(x_c)\right] \tag{A5}$$

where $B_{nl}$is the normalization constant and $\rho(x_c)$the weight function which satisfies the condition below;

$$(\sigma(x_c)\,\rho(x_c))'=\tau(x_c)\,\rho(x_c) \tag{A6}$$

where also

$$\tau(x_c)=\tilde{\tau}(x_c)+2\pi(x_c) \tag{A7}$$

For bound solutions, it is required that

$$\tau'(x_c)<0 \tag{A8}$$

The eigenfunctions and eigenvalues can be obtained using the definition of the following function $\pi(s)$ and parameter λ, respectively:

$$\pi(s)=\frac{\sigma'(s)-\tilde{\tau}(s)}{2}\pm\sqrt{\left(\frac{\sigma'(s)-\tilde{\tau}(s)}{2}\right)^2-\tilde{\sigma}(s)+k\sigma(s)} \tag{A9}$$

and

$$\lambda=k_-+\pi'_-(x_c) \tag{A10}$$

The value of *k* can be obtained by setting the discriminant in the square root in Eq. (A9) equal to zero. As such, the new eigenvalues equation can be given as

$$\lambda+n\tau\prime(x_c)+\frac{n(n-1)}{2}\sigma\prime\prime(x_c)=0,(n=0,1,2,\ldots) \tag{A11}$$

Received: 2 May 2024; Accepted: 5 November 2024
Published online: 27 March 2025

References

1. William, E. S. et al. Magnetic susceptibility and magnetocaloric effect of Frost-Musulin potential subjected to magnetic and Aharonov-Bohm(Flux)for CO and NO diatomic molecules. *J. Theoretical Appl. Phys.* **17** (2,12), 172318. https://doi.org/10.30495/JTAP.172318 (2023).
2. Inyang, E. P. et al. The effect of topological defect on the mass spectra of heavy and heavy-light Quarkonia. *Eurasian Phys. Tech. J.* **19** (42), 87. https://doi.org/10.31489/2022No4/78-87 (2022).
3. Inyang, E. P. et al. Analytic study of thermal properties and masses of heavy mesons with quarkonium potential. *Res. Phys.* https://doi.org/10.1016/j.rinp.2022.105754 (2022).
4. Inyang, E. P. & Okon, I. B. Quantum mechanical treatment of Shannon Entropy measure and energy spectra of selected diatomic molecules with the modified Kratzer plus generalized inverse quadratic Yukawa potential model. *J. Theoretical Appl. Phys.* **17**, 4, 172340. https://doi.org/10.57647/j.jtap.2023.1704.40 (2023). ·William, E. S.·Okoi, P. O. & Ibanga, E. A
5. Obu, J. A., William, E. S., Akpan, I. O., Thompson, E. A. & Inyang, E. P. Analytical Investigation of the single-particle energy spectrum in magic nuclei of 56Ni and 116Sn. *Eur. J. Appl. Phys.* **2**, 1 (2020).
6. Obu, J. A. et al. The effect of Debye mass on the mass spectra of Heavy Quarkonium system and its thermal properties with class of Yukawa potential. *Jordan J. Phys.* **16** (3), 339. https://doi.org/10.47011/16.3.8 (2023).
7. Inyang, E. P., Ali, N., Endut, R., Rusli, N. & Aljunid, S. A. The radial scalar power potential and its application to quarkonium systems. *Indian J. Phys.* https://doi.org/10.1007/s12648-024-03335-9 (2024).
8. Inyang, E. P. et al. Application of Eckart-Hellmann potential to study selected diatomic molecules using Nikiforov-Uvarov-Functional analysis method. *Rev. Mex. Fis.* **68**, 14 (2022).
9. Omugbe, E. et al. Non-relativistic energy spectra of and diatomic molecules confined in a modified scarf potential via supersymmetric WKB approach, Molecular Physics,(2024). https://doi.org/10.1080/00268976.2024.2390591
10. William, E. S. et al. Ro-vibrational energies and expectation values of selected diatomic molecules via Varshni plus modified Kratzer potential model. *Indian J. Phys.* https://doi.org/10.1007/s12648-0222-02308-0 (2022).
11. Inyang, E. P., Omugbe, E., Abu-shady, M. & William, E. S. Investigation of Quantum Information Theory with the screened modified Kratzer and a class of Yukawa potential model. *Eur. Phys. J. Plus* **138**, 969. https://doi.org/10.1140/epjp/s13360-023-04617-7 (2023).
12. Ayedun, F., Inyang, E. P., EIbanga, A. & Lawal, K. M. Analytical Solutions to the Schrödinger equation with collective potential models: application to Quantum Information Theory. *East. Eur. J. Phys.* **4** https://doi.org/10.26565/2312-4334-2022-4-06 (2022).

13. Inyang, E. P. et al. Information entropies with Varshni-Hellmann potential in higher dimensions. *Phys. Open.* **100220** https://doi.org/10.1016/j.physo.2024.100220 (2024).
14. Amadi, P. O. et al. Shannon Entropy and Fisher information for screened Krattzer potential. *Int. J. Quantum Chem.* e26246,(2020).
15. Shannon, C. E. A Mathematical theory of communication. *Bell Syst. Tech. J.* **27** https://doi.org/10.1002/j.1538-7305.1948.tb01338.x (1948).
16. Santana-Carrillo, R., Peto, J. M. V., Sun, G. H. & Dong, S. H. Quantum information entropy for a hyperbolic DoubleWell potential in the fractional Schrödinger equation. *Entropy* **25**, 988. https://doi.org/10.3390/e25070988 (2023).
17. Ikot, A. N. et al. Quantum information-entropic measures for exponential-type potential. *Res. Phys.* **103150** https://doi.org/10.1016/j.rinp.2020.103150 (2020).
18. Inyang, E. P. et al. Quantum mechanical treatment of Shannon entropy measure and energy spectra of selected diatomic molecules with the modified Kratzer plus generalized inverse quadratic Yukawa potential model.*J. Theor. Appl. Phys.* **17**, 4, 172340 (2023). https://doi.org/10.57647/j.jtap.2023.1704.40
19. Fisher, R. A. Theory of statistical estimation. *Proc. Camb. Philosphical Soc.* **22** (700). https://doi.org/10.1017/S0305004100009580 (1925).
20. Sears, S. B., Parr, R. G. & Dinur, U. On the Quantum-mechanical kinetic energy as a measure of the information in a distribution. *Isreal J. Chem.* **19**, 165. https://doi.org/10.1002/ijch.198000018 (1980).
21. Omugbe, E. et al. Fisher information entropies and the strength of an oscillator under a mixed hyperbolic Pöschl–Teller potential function. *Indian J. Phys.* **97**, 3411. https://doi.org/10.1007/s12648-023-02676-1 (2023).
22. Isonguyo, C. N., Oyewumi, K. J. & Oyun, O. S. Quantum information-theoretic measures for the static screened Coulomb potential int. *J. Quant. Chem.* **118**, 025620 (2018).
23. Nagy, A. Fisher and Shannon information in orbital-free density functional theory. *Int. J. Quantum Chem.* **115**, 1392 (2015).
24. Okon, I. B. et al. N.Thermomagnetic properties and its efects on Fisher entropy with Schioberg plus ManningRosen potential (SPMRP) using NikiforovUvarov functional analysis (NUFA) and supersymmetric quantum mechanics (SUSYQM) methods. *Sci. Rep.* **13**, 8193. https://doi.org/10.1038/s41598-023-34521-0 (2023).
25. Wang, Z. et al. Synchronization patterns in a network of diffusively delay-coupled memristive Chialvo neuron map. *Phys. Lett. A* **514**, 129607. https://doi.org/10.1016/j.physleta.2024.129607 (2024).
26. Wang, Z., Chen, M., Xi, X., Tian, H. & Yang, R. Multi-chimera states in a higher order network of FitzHugh–Nagumo oscillators.*Eur. Phys. J. Special Topics* **233** (4), 779 (2024). doi: (2024). https://doi.org/10.1140/epjs/s11734-024-01143-0
27. Ali, T. A. A., Xiao, Z., Jiang, H. & Li, B. A. Class of Digital integrators based on trigonometric quadrature rules. *IEEE Trans. Industr. Electron.* **71** (6), 6128–6138. https://doi.org/10.1109/TIE.2023.3290247 (2024).
28. Dong, J., Hu, J., Zhao, Y. & Peng, Y. Opinion formation analysis for expressed and private opinions (EPOs) models: reasoning private opinions from behaviors in group decision-making systems. *Expert Syst. Appl.* **236**, 121292. https://doi.org/10.1016/j.eswa.2023.121292 (2024).
29. Peng, Y., Zhao, Y. & Hu, J. On the role of community structure in evolution of opinion formation: a new bounded confidence opinion dynamics. *Inf. Sci.* **621**, 672. https://doi.org/10.1016/j.ins.2022.11.101 (2023).
30. Wu, M., Wang, B., Ba, Z., Dai, K. & Liang, J. Propagation attenuation of elastic waves in multi-row infinitely periodic pile barriers: a closed-form analytical solution. *Eng. Struct.* **315**, 118480. https://doi.org/10.1016/j.engstruct.2024.118480 (2024).
31. Lin, S., Zhang, J. & Qiu, C. Asymptotic analysis for one-stage stochastic linear complementarity problems *Appl. Math.* **11**(2), 482 doi: https://doi.org/10.3390/math11020482 (2023).
31. Xiang, X., Zhou, J., Deng, Y. & Yang, X. Identifying the generator matrix of a stationary Markov chain using partially observable data. *Chaos: Interdisciplinary J. Nonlinear Sci.* **34**, 023132. https://doi.org/10.1063/5.0156458 (2024).
32. Zhang, X., Hu, Z. & Liu, Y. Fast generation of GHZ-like States using collective-spin XYZ Model. *Phys. Rev. Lett.* **132** (11), 113402. https://doi.org/10.1103/PhysRevLett.132.113402 (2024).
33. Hou, X. et al. A self-powered biomimetic mouse whisker sensor (BMWS) aiming at terrestrial and space objects perception. *Nano Energy* **118**, 109034. https://doi.org/10.1016/j.nanoen.2023.109034 (2023).
34. Hou, X. et al. A space crawling robotic bio-paw (SCRBP) enabled by triboelectric sensors for surface identification. *Nano Energ.* **105**, 108013. https://doi.org/10.1016/j.nanoen.2022.108013 (2023).
35. Omugbe, E. et al. Information-theoretic measures and thermodynamic properties under magnetic and aharonov–bohm flux Fields. *Eur. Phys. J. D* **77**, 143. https://doi.org/10.1140/epjd/s10053-023-00718-1 (2023).
36. Omugbe, E. et al. Non- relativistic bound state solutions with -deformed Kratzer-type potential using the super-symmetric WKB method: application to theoretic-information measures. *Eur. Phys. J. D* **76,72**, 11 (2022).
37. Boumali, A. & Labidi, M. The solutions on one-dimensional Dirac oscillator with energy-dependent potentials and their effects on the Shannon and Fisher quantities of quantum information theory. *J. Low Temp. Phys.* **204**, 47. https://doi.org/10.1007/s10909-021-02596-6 (2021).
38. Martanez-Flores, C. Shannon Entropy and Fisher information for endohedral confined one- and two-electron atoms. *Phys. Lett. A* **386**, 126988. https://doi.org/10.1016/j.physleta.2020.126988 (2021).
39. Dong, S., Sun, G-H., Dong, S-H. & Draayer, J. P. Quantum information entropies for a squared tangent potential well. *Phys. Lett. A*. **378**, 130 (2014).
40. Song, X-D., Dong, S-H. & Zhang, Y. Quantum information entropy for one-dimensional system undergoing quantum phase transition. *Chin. Phys. B*, **25**, 5, (2016).
41. Gil-Barrera, C. A., Santana Carrillo, R., Sun, G. H. & Dong, S. H. Quantum information entropies on hyperbolic single potential Wells. *Entropy* **24**, 604. https://doi.org/10.3390/e24050604 (2022).
42. El-Qahtani, M. H., Berrada, K., Abdel-Khalek, S. & Eleuch, H. Thermal Fisher information and entropy squeezing for superconducting qubits. *Res. Phys.* **39**, 105639 (2022).
43. Abdelmonem, M. S., Abdel-Hady, A., Nasser, I. & M.& Information entropies for the Morse potential using the J-matrix method. *Res.Phys.* **7**, 1780 (2017).
44. Edet, C. O., Lima, F. C. E., Almeida, C. A. S., Ali, N. & Asjad, M. Quantum information of the Aharanov-Bohm ring with Yukawa interaction in the presence of disclination, Entropy 24,1059,(2022).
45. Ikot, A. N. et al. Quantum information-entropic measures for exponential – type potential. *Res. Phys.* **18**, 103150 (2020).
46. Ikot, A. N. et al. Theoretic quantum information entropies for the generalized hyperbolic potential. *Int. J. Quantum Chem.*, e26410,(2020).
47. (2023). doi:https://doi.org/10.1016/j.rinp.2023.107037.
48. Zhu, C. et al. Analytical study of nonlinear models using a modified Schrödinger equation and logarithmic transformation. *Res. Phys.* **55**, 107183. https://doi.org/10.1016/j.rinp.2023.107183 (2023).
49. Zhu, C., Al-Dossari, M., El-Gawaad, N. S. A., Alsallami, S. A. M. & Shateyi, S. Uncovering diverse soliton solutions in the modified Schrödinger's equation via innovative approaches. *Results Phys.* **54**, 107100. https://doi.org/10.1016/j.rinp.2023.107100 (2023).
50. Zhu, C., Abdallah, S. A. O., Rezapour, S. & Shateyi, S. On new diverse variety analytical opticalsoliton solutions to the perturbed nonlinear Schrödinger equation. *Res. Phys.* **54**, 107046. https://doi.org/10.1016/j.rinp.2023.107046 (2023).
51. Kai, Y. & Yin, Z. On the gaussian traveling wave solution to a special kind of Schrödinger equation with logarithmic nonlinearity. *Mod. Phys. Lett. B* **36** (02), 2150543. https://doi.org/10.1142/S0217984921505436 (2021).
52. Inyang, E. P. et al. Thermal properties, Mass spectra and root mean square radii of heavy quarkonium system with class of inversely quadratic Yukawa Potential. *AIP Conf. Proc.* **2679** (030003). https://doi.org/10.1063/5.0112829 (2023).

53. Nikiforov, S. K. & Uvarov, V. B. *Special Functions of Mathematical Physics* (Birkhauser, 1988).
54. William, E. S., Inyang, E. P. & Thompson, E. A. Arbitrary-solutions of the Schrödinger equation interacting with Hulthen-Hellmann potential model. *Rev. Mex. Fis.* **66** (6), 741 (2020).
55. Inyang, E. P., William, E. S. & Obu, J. A. Eigensolutions of the N-dimensional Schrödinger equation interacting with Varshni-Hulthen potential model. *Revista Mexicana de Fisica* **67**(2)193((2021).
56. Abramowitz, M. & Stegun, I. A. *Handbook of mathematical functions with formulas, graphs, and mathematical tables*, U.S. Department of commerce, National bureau of standards: New York ,(1965).
57. Ikhdair, S. M. Approximate l-states of the Manning-Rosen potential by using Nikiforov-Uvarov method. *Int. Sch. Res. Notices* (2012).
58. Inyang, E. P., Inyang, E. P., William, E. S., Ntibi, J. E. & Ibanga, E. A.Bound State solutions of the Schrödinger equation with Frost-Musulin potential using the Nikiforov-Uvarov-Functional Analysis (NUFA) method. *Bulg. J. Phys.*, **20**,11 (2022).
59. Edet, C. O. & Ikot, A. N. Shannon information entropy in the Presence of magnetic and Aharanov-Bohm(AB) fields. *Eur. Phys. J. Plus* ,136,432,(2021).
60. Bialynicki-Birula, I. & Mycielski, J. Uncertainty relations for information entropy in wave mechanics. *Commun. Math. Phys.* **44** https://doi.org/10.1007/BF01608825 (1975). ,129,.
61. Patil, S. H., Sen, K. D., Watson, N. A. & Montgomery, H. E. Characteristic features of net information measures for constrained Coulomb potentials. *J. Phys. B: at. Mol. Opt. Phys.* **40**, 11,2147,2007).
62. Chakraborty, D. & Ayers, W. *Statistical complexity: Applications in electronic structure*(Ed:K.D.Sen)Springer, (2012).
63. Romera, E., Sánchez-Moreno, P. & Dehesa, J. S. The Fisher information of single-particle systems with a central potential. *Chem. Phys. Lett.* **414**, 6,472, (2005).
64. Inyang, E. P. et al. Energy Spectra and expectation values of selected diatomic molecules through the solutions of Klein-Gordon equation with Eckart-Hellmann potential model. *Mol. Phys.* **119** (23), e1956615. https://doi.org/10.1080/00268976.2021.1956615 (2021).
65. Inyang, E. P. et al. Analytical Solutions of the N-Dimensional Schrödinger equation with modified screened Kratzer plus inversely quadratic Yukawa potential and thermodynamic properties of selected diatomic molecules. *Res. Phys.*. (2022). https://doi.org/10.1016/j.rinp.2022.106075
66. Inyang, E. P. et al. Expectation values and energy spectra of the varshni potential in arbitrary dimensions.*Jordan J. Phys.* 5 509 (2022)
67. Begui, M. & Meftah, M. T. Ground state energy for confined diatomic molecules: case of Morse interaction. *Mol. Phys.* **122** (3), e2251611 (2024).
68. Ibekwe, E. E., Okorie, U. S., Emah, J. B., Inyang, E. P. & Ekong, S. A. Mass spectrum of heavy quarkonium for screened Kratzer potential (SKP) using series expansion method. *Eur. Phys. J. Plus* **136**, 11 (2021).
69. Bayrak, O. R. H. A. N., Boztosun, I. & Ciftci, H. A. K. A. N. Exact analytical solutions to the Kratzer potential by the asymptotic iteration method. *Int. J. Quantum Chem.* **107** (3), 540 (2007).
70. Inyang, E. P. & Obisung, E. O. The study of electronic states of NI and ScI molecules with screened Kratzer potential. *East. Eur. J. Phys.* **3** https://doi.org/10.26565/2312-4334-2022-3-04 (2022).
71. Heisenberg, W. Quantum-theoretical re-interpretation of kinematic and mechanical relations. *Z. Phys.* **33**, 893 (1925).
72. Francis, M. N., Peierls, R. E. W. & Heisenberg 5, 251 (1977).
73. Ntibi, J. E., Inyang, E. P., Inyang, E. P. & William, E. eddy Relativistic treatment of D-dimensional Klein-Gordon equation with Yukawa potential. *Int.J. Innovative Sci. Eng. Technol.*, 7(11) (2020). https://ijiset.com/vol7/v7s11/IJISET_V7_I11_04.pdf
74. Ghasemi, A., Hooshmandasl, M. R. & Tavassoly, M. K. On the quantum information entropies and squeezing associated with the eigenstates of the isotonic oscillator. *Phys. Scr.* **84** (3), 035007 (2011).
75. Pooja, A. S., Gupta, R. & Kumar, A. Quantum information entropy of modified Hylleraas plus exponential Rosen Morse potential and squeezed states. *Int. J. Quantum Chem.* **117**, 11, e25368 (2017).
76. Bayrak, O., Boztosun, I. & Ciftci, H. Exact analytical solutions to the Kratzer potential by the asymptotic iteration method. *Int. J. Quantum Chem.* **107** (3), 540 (2007).
77. Inyang, E. P. et al. Approximate solutions of the Schrödinger equation with Hulthén plus screened Kratzer potential using the Nikiforov–Uvarov–functional analysis (NUFA) method: an application to diatomic molecules. *Can. J. Phys.* **100** (10), 463–473 (2022).
78. Vigo-Aguiar, J. & Simos, T. E. Review of multistep methods for the numerical solution of the radial Schrödinger equation. *Int. J. Quantum Chem.* **103** (3), 278 (2005).
79. Inyang, E. P., William, E. S., Ibanga, E. A., Ntibi, J. E. & Akintola, O. O. Bound state solutions to the Schrodinger equation for selected Diatomic Molecules. *J. Nigerian Assoc. Math. Phys.* **64**, 12 (2022).
80. Song, X. D., Dong, S-H. & Zhang, Y. Quantum information entropy for one-dimensional system undergoing quantum phase transition. *Chin. Phys. B* **25**, 5,050302 (2016).
81. Valencia-Torres, R., Sun, G-H. & Dong, S-H. Quantum information entropy for a hyperbolical potential function. *Phys. Scr.* **90** (3), 035205 (2015).

Acknowledgements

N. Ali, Inyang, E.P. and A.E.L. Aouami, acknowledges the support from the UniMAP Special Research Grant-International Postdoctoral with grant number: 9004-00100. The authors are grateful to the editorial team of the journal and the reviewers for their positive comments and suggestions, which have been used to further improve the quality of this manuscript. This work was supported by the Ministry of Higher Education of Malaysia (Funding No. LRGS/1/2020/UM/01/5/2 Fault-tolerant Photonic Quantum States for Quantum Key Distribution) and Universiti Malaysia Perlis (Funding No. 9004-00100 Special Research Grant-International Postdoctoral).

Author contributions

Inyang E. P., A.E.L. Aouami, and Ali N. formulated the problem, wrote the full manuscript, and presented the results and graphics.Ali N. R. , and Endut R. performed computational analysis. Aljunid S.A. progresses by creating the literature, carefully reviewing it, and making essential revisions to the manuscript. All authors have reviewed and endorsed the final manuscript.

Funding

This research was carried out under LRGS Grant LRGS/1/2020/UM/01/5/2 (9012-00009), Fault-tolerant Photonic Quantum States for Quantum Key Distribution, provided by the Ministry of Higher Education of Malaysia (MOHE). The authors are grateful for the financial support received from the UniMAP UniPrima Research Grant 9002 – 00160.

Declarations

Competing interests
The authors declare no competing interests.

Dedication
Dr. Etido P. Inyang respectfully dedicates this research to his late father, who was lead to rest on July 20, 2024.

Additional information
Correspondence and requests for materials should be addressed to E.P.I. or R.E.

Reprints and permissions information is available at www.nature.com/reprints.

Publisher's note Springer Nature remains neutral with regard to jurisdictional claims in published maps and institutional affiliations.